Journal of Pharmacokinetics and Pharmacodynamics (2019) 46:15–25
https://doi.org/10.1007/s10928-018-9612-y

ORIGINAL PAPER

Benchmarking renin suppression and blood pressure reduction of direct renin inhibitor imarikiren through quantitative systems pharmacology modeling

Yeshitila Gebremichael[1] · Gezim Lahu[2] · Majid Vakilynejad[3] · K. Melissa Hallow[1]

Received: 9 April 2018 / Accepted: 1 November 2018 / Published online: 16 November 2018

Abstract

Multiple classes of antihypertensive drugs inhibit components of the renin–angiotensin–aldosterone system (RAAS). The primary physiological effector of the RAAS is angiotensin II (AngII) bound to the AT1 receptor (AT1-bound AngII). There is a strong non-linear feedback from AT1-bound AngII on renin secretion. Since AT1-bound AngII is not readily measured experimentally, plasma renin concentration (PRC) and/or activity (PRA) are typically measured to indicate RAAS suppression. We investigated the RAAS suppression of imarikiren hydrochloride (TAK-272; SCO-272), a direct renin inhibitor currently under clinical development. We employed a previously developed quantitative system pharmacology (QSP) model to benchmark renin suppression and blood pressure regulation with imarikiren compared to other RAAS therapies. A pharmacokinetic (PK) model of imarikiren was linked with the existing QSP model, which consists of a mechanistic representation of the RAAS pathway coupled with a model of blood pressure regulation and volume homeostasis. The PK and pharmacodynamic effects of imarikiren were calibrated by fitting drug concentration, PRA, and PRC data, and trough AT1-bound AngII suppression was simulated. We also prospectively simulated expected mean arterial pressure reduction in a cohort of hypertensive virtual patients. These predictions were benchmarked against predictions for several other (previously calibrated) RAAS monotherapies and dual-RAAS therapies. Our analysis indicates that low doses (5–10 mg) of imarikiren are comparable to current RAAS therapies, and at higher doses (25–200 mg), RAAS suppression may be equivalent to existing dual-RAAS combinations (at registered doses). This study illustrates application of QSP modeling to predict phase II endpoints from phase I data.

Keywords Direct renin inhibitor · Quantitative systems pharmacology · Antihypertensive drugs · RAAS · Renal physiology model

Introduction

Abnormal perturbations of the renin–angiotensin–aldosterone system (RAAS) are associated with cardiovascular and renal complications. In particular, the RAAS is related to essential and secondary forms of hypertension, making the RAAS pathway a major target for therapeutic intervention. The enzyme renin is synthesized as prorenin in the juxtaglomerular (JG) cells in the kidney, and secreted as either renin or prorenin [1]. Although JG cells are the primary renin producers, other tissues have been shown to form prorenin as well [1, 2]. Renin cleaves angiotensinogen to form the biologically inactive peptide angiotensin I (AngI). AngI is in turn hydrolyzed by angiotensin-converting enzyme (ACE) and chymase to form angiotensin II (AngII), the primary biologically active peptide of the RAAS pathway. Other branches in the pathway lead to formation of Ang (1–7), AngIV, and other angiotensins, as recently reviewed [3], but the physiologic role of these peptides is less well understood. AngII is a potent vasoconstrictor that plays a critical role in blood pressure

✉ Yeshitila Gebremichael
ygebremichael@dilisym.com

[1] School of Chemical, Materials and Biomedical Engineering, College of Engineering, University of Georgia, Athens, GA, USA

[2] thinkQ2 AG, Baar, Switzerland

[3] Takeda Pharmaceuticals U.S.A., Inc., Deerfield, IL, USA

regulation through arterial vasoconstriction, sympathetic nervous system stimulation, increased aldosterone secretion, and altered renal sodium handling [4]. These actions of AngII are primarily mediated through type 1 (AT1) receptor binding [5]. AngII may also elicit action through binding to the type 2 (AT2) receptors. These receptors may counteract the effects of AT1, for example by promoting vasodilation or reducing inflammation [6], but the physiological significance of AT2 receptors remains a topic of investigation [7, 8].

Therapies that target various parts of the RAAS pathway are vital in treating hypertensive disorders. Angiotensin receptor blockers (ARBs) act downstream by inhibiting AT1 receptors [9]. ACE inhibitors (ACEi) block the pathway in the middle, inhibiting AngII formation by blocking ACE. Direct renin inhibitors (DRIs) block the pathway upstream by deactivating renin, preventing the conversion of angiotensinogen to AngI that initiates the RAAS cascade. ACEi or ARBs trigger a reactive feedback mechanism that increases plasma renin activity [10], causing a compensatory increase in AngI and/or AngII, partially restoring downstream blockades of the RAAS [10]. While renin inhibitors also elicit large increases in renin secretion [11], the excess renin secreted is largely inactivated, so that AngI and AngII remain suppressed [12]. In addition, renin inhibition is attractive because of the specificity of renin to its substrate (renin is highly selective to angiotensinogen whereas, e.g., ACE binds to bradykinin in addition to AngI [13]).

Among DRIs, aliskiren was the first orally bioavailable DRI approved by the US Food and Drug Administration (FDA). Imarikiren is another novel potent and orally active DRI currently under development for treatment of diabetic nephropathy and hypertension. Imarikiren is reported to have better oral bioavailability in rats than aliskiren (25.2% vs. 2.4%) [14]. The improvement in bioavailability is thought to arise from better physiochemical characteristics (such as molecular weight, topological polar surface area and number of rotatable bonds) related to bioavailability [14].

Since most known pathophysiological effects of ANGII are mediated through AT1 receptors, all of these drugs primarily produce physiologic effects by suppressing AT1-bound AngII (although there are potentially secondary effects through Ang (1–7) and AT2-bound AngII). The degree of AT1-bound AngII suppression is expected to determine the physiological effects, but AT1-bound AngII cannot be measured directly. Measurements of circulating AngI and AngII peptides is also challenging due to assay sensitivity to sample extraction and handling and assay conditions [15]. Plasma renin activity (PRA) and plasma renin concentration (PRC) can be measured with greater precision (although in most assays there is lower limit of quantification for PRA that makes low level detection challenging). However, when AT1-bound AngII is suppressed, there is a non-linear feedback on renin secretion, making it more challenging to benchmark RAAS suppression based on PRA and PRC directly.

We have previously published a mathematical model of the RAAS pathway that includes the nonlinear feedback between AT1-bound AngII and renin secretion [16, 17]. The RAAS pathway model also feeds into a larger cardio-renal QSP model of blood pressure regulation and fluid and electrolyte homeostasis [17, 18]. The model has been previously developed and validated for several classes of antihypertensive agents targeting the RAAS pathway [17]. Here, we apply this model to the new orally bioavailable renin inhibitor imarikiren. We show that the model is capable of reproducing the observed temporal changes of PRA and PRC arising from imarikiren administration. We then benchmark the trough suppression of AT1-bound AngII against other RAAS targeting agents, and predict expected trough mean arterial pressure reduction.

Methods

Clinical data

As part of Phase I clinical study, single ascending doses of 5, 10, 25, 50, 100 and 200 mg imarikiren were administered orally to healthy adult male volunteers (n = 8 for each group except for 50 mg, where n = 20). A placebo group (n = 12) was also included. For each dose, the concentration–time profile of imarikiren were measured initially every half hour and then at longer intervals through day 7. Additionally, among others, plasma PRA and PRC were measured at frequent intervals through day 7.

Mathematical model

We employed a previously developed QSP model [16–18] that consists of three interlinked components, as illustrated in Fig. 1: a pharmacokinetic/pharmacodynamics (PK/PD) model, a model of the RAAS pathway, and a cardio-renal model of blood pressure regulation and volume homeostasis. The pharmacokinetics of imarikiren drives changes in renin activity in the RAAS pathway model, leading to changes in AT1-bound AngII and MR-bound aldosterone, which are linked to downstream physiological effects in the cardio-renal model that leads to changes in blood pressure.

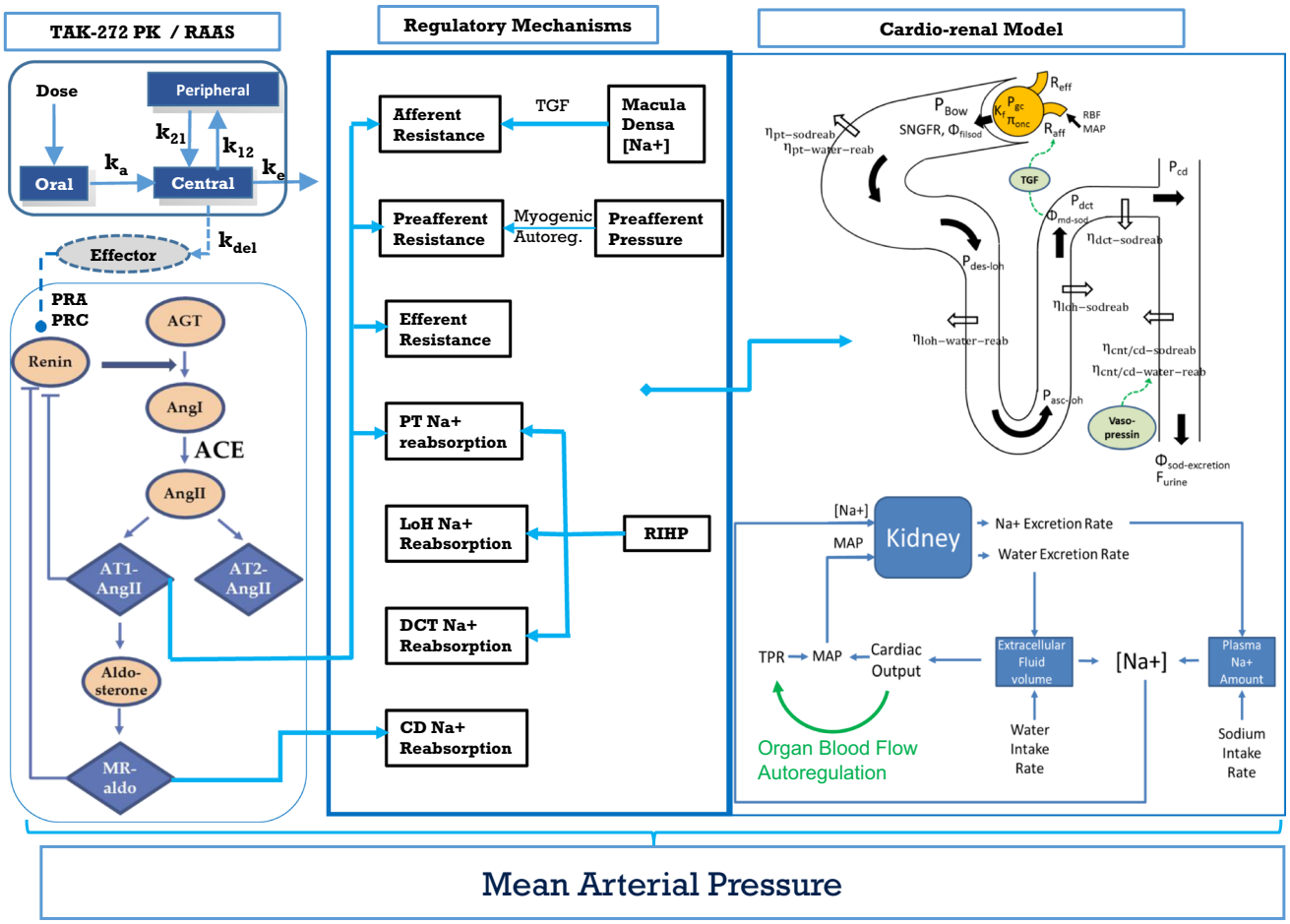

Fig. 1 The QSP model consists of a mechanistic model of the RAAS pathway coupled with a model of the cardio-renal system and blood pressure regulation. A two-compartment PK model (left column, top) dynamically drives renin inhibition and subsequent suppression of downstream RAAS components (left column, bottom). AT1-bound AngII and aldosterone in the RAAS model trigger downstream regulatory effects of vasoconstriction and tubular sodium reabsorption (middle column), which in turn lead to blood pressure regulation through the cardio-renal model (right column). The QSP model is described in detail in Refs. [16–18, 20, 21]

PK/PD model of imarikiren

A two-compartment PK model was used to characterize the plasma concentration profile of imarikiren at all doses. Nonlinear distribution and elimination terms, as described for other renin inhibitors [19], were evaluated, but did not significantly improve the model fit. Thus, first-order linear terms were used.

The pharmacodynamic (PD) effect of imarikiren on renin inhibition was described with a sigmoidal E_{max} model. An effect compartment was used to account for time lag between exposure and renin inhibition. The effect compartment concentration $[IMAR_{eff}]$ was modeled as

$$\frac{d}{dt}\left([IMAR_{eff}]\right) = k_{del}\left([IMAR] - [IMAR_{eff}]\right) \quad (1)$$

where $[IMAR]$ is the concentration of imarikiren in the central compartment and k_{del} is the first order distribution rate constant that determines the time lag for drug action.

The effect of imarikiren on PRA inhibition was then calculated as

$$PRA_{inhibition} = 1 - \frac{E_{\max}[IMAR_{eff}]}{[IMAR_{eff}] + IC50} \quad (2)$$

where the model parameters E_{max} and $IC50$ are the maximum possible drug effect and the drug concentration producing half maximum effect, respectively.

RAAS pathway model

The RAAS pathway submodel has been described in detail previously [17]. The model was previously developed and calibrated by fitting the trough PRA and PRC responses to various monotherapies targeting the RAAS, and then validated by simulating the trough PRA and PRC responses to these drugs in combination. Key model equations that describe the RAAS cascade are briefly described below.

As mentioned above, AngI is formed by PRA, assuming that its precursor angiotensinogen is available in excess and the active plasma renin is the rate-limiting factor. AngI is converted to AngII by the enzymes ACE and chymase, and is degraded at a rate of $K_{d,AngI}$. The differential equation describing the rate of change of AngI is expressed as

$$\frac{d[AngI]}{dt} = PRA - \left(K_{ace} + K_{chymase}\right)[AngI] - K_{d,AngI}[AngI] \tag{3}$$

AngII is formed from the action of ACE and chymase on AngI at the rate K_{ace} and $K_{chymase}$, respectively. The peptide binds to either the AT1 or AT2 receptors at the rate K_{AT1} and K_{AT2} respective, and is degraded at a rate of $K_{d,AngII}$. The equation describing the rate of change of AngII is given as

$$\begin{aligned}\frac{d[AngII]}{dt} &= \left(K_{ace} + K_{chymase}\right)[AngI] \\ &-(K_{AT1} + K_{AT2})[AngII] - K_{d,AngII}[AngII]\end{aligned} \tag{4}$$

The complex of AngII bound to the AT1 receptor ($AT1_{bound}AgnII$) is the physiologically active entity within the RAAS pathway, and is determined by the relation

$$\frac{d[AT1_{bound}AngII]}{dt} = K_{AT1}[AngII] - K_{d,AT1}[AT1_{bound}AngII] \tag{5}$$

where $K_{d,AT1}$ is the degradation rate constant for AT1-bound AngII.

AT1-bound AngII also induces aldosterone secretion. The aldosterone secretion rate Sec_{aldo} and aldosterone concentration are modeled as

$$\begin{aligned}Sec_{aldo} = Sec_{aldo,0}\big(1 + m_{AT1-aldo}\big(&\left[AT1_{bound}AngII\right] \\ &- [AT1_{bound}AngII_0]\big)\big)\end{aligned} \tag{6}$$

$$\frac{d[Aldosterone]}{dt} = Sec_{aldo} - K_{d,aldo}[Aldosterone] \tag{7}$$

$Sec_{aldo,0}$ is the nominal rate of aldosterone secretion. [AT1-bound $AngII_0$] is the nominal AT1-bound AngII. $m_{AT1\text{-}aldo}$ is a linear fitting constant. $K_{d,aldo}$ is the aldosterone degradation rate constant.

Renin secretion feedback mechanism AT1-bound AngII exerts a strong inhibitory effect on renin secretion, and suppression of AT1-bound AngII stimulates large, nonlinear increases in renin secretion. In addition, renin secretion is altered by sodium flow through the macula densa. Renin is assumed to be secreted at a nominal rate $SEC_{renin,0}$ and is modulated by feedback signals arising from sodium flow at the macula densa ($\mu_{md-renin}$) as well as a feedback signal μ_{AT1} arising from AT1 binding to AngII. As a result, the renin secretion rate SEC_{renin} is expressed as

$$SEC_{renin} = \mu_{md-renin}\mu_{AT1}SEC_{renin,0} \tag{8}$$

Circadian variation in renin secretion was not considered in this analysis.

We previously showed that the inhibitory effect of AT1-bound AngII on renin secretion can be well characterized by the relationship [17]

$$\mu_{AT1} = \left(\frac{[AT1_{bound}AngII]}{[AT1_{bound}AngII_0]}\right)^{-A_{AT1,ren}} \tag{9}$$

The exponent $A_{AT1,ren}$ is a fitting constant.

The feedback signal due to macula densa sodium flow, $\mu_{md-renin}$ is a function of the macula densa sodium concentration $\phi_{Na,md}$, which is calculated in the cardio-renal submodel, described later.

$$\mu_{md-renin} = \exp\left(-A_{md-ren}\left(\phi_{Na,md} - \phi_{Na,md,0}\right)\right) \tag{10}$$

$\phi_{Na,md,0}$ is the normal macula densa sodium concentration under baseline conditions and A_{md-ren} is a fitting constant.

Under the conditions considered in this study, macula densa sodium changes are relatively small, while changes in AT1-bound AngII in response to RAAS blockade are quite large. Thus, the feedback on renin secretion is dominated by μ_{AT1}.

The rate of change of PRC is determined in terms of renin secretion and degradation rate $K_{d,renin}$ as:

$$\frac{d(PRC)}{dt} = SEC_{renin} - K_{d,renin} * PRC \tag{11}$$

PRA is assumed to be linearly proportional to PRC with a scaling factor k, and is modulated by drug-induced PRA inhibition factor $PRA_{inhibition}$ according to the relation

$$PRA = k * PRC * (1 - PRA_{inhibition}) \tag{12}$$

$PRA_{inhibition}$ is the pharmacodynamical effect of imarikiren as described in Eq. 2.

Cardio-renal systems model for blood pressure regulation

We employed a previously described cardio-renal systems model [17] to link imarikiren administration and the resulting RAAS suppression to the physiologic effects of the RAAS, in order to predict the expected mean arterial pressure response. The model describes the physiological processes of volume and blood pressure regulation through renal filtration, reabsorption, and excretion, including multiple regulatory mechanisms. These regulatory

mechanisms include intrinsic mechanisms like tubuloglomerular feedback (TGF) and neurohormonal mechanisms like the RAAS cascade, for simultaneous control of Na + homeostasis, stable cardiac output, mean arterial pressure (MAP), glomerular pressure or glomerular filtration rate (GFR), and others. A detailed description of the cardio-renal model and its feedback mechanisms along with tubular Na + and water reabsorption processes are described in Refs. [17, 18, 20, 21]. Here we present only the links between the RAAS pathway submodel and its physiologic effects.

For therapeutic agents that target the RAAS, the ultimate consequence is suppression of AT1-bound AngII. AT1-bound AngII in turn has multiple physiologic effects, including constriction of the efferent, preglomerular, afferent, and systemic vasculature, sodium retention in the proximal tubule, and aldosterone secretion. The model captures each of these effects through feedback mechanism that scales the physiologic effect by changes in AT1-bound AngII according to the relation

$$M_{AT1,i} = 1 + S_{AT1,i} * \left(\frac{1}{1 + \exp\left(\frac{[AT1_{bound} AngII_0] - [AT1_{bound} AngII]}{m_{AT1,i}} \right)} - 0.5 \right) \quad (13)$$

where i represents the effect on efferent, afferent, preafferent, or systemic resistance, proximal tubule sodium reabsorption, or aldosterone secretion. The effect of drug-induced changes in AT1-bound AngII on each of these physiological variables results in blood pressure reduction as described in detail by Hallow et al. [17, 18, 20, 21]. As previously described [17], this portion of the model was validated by simulating the trough mean arterial pressure reduction observed in clinical studies of 4–8 weeks treatment with ARBs (candesartan, irbesartan, losartan, and valsartan), ACE inhibitors (enalapril, ramipril), aliskiren, and the combination of aliskiren with valsartan or ramipril. The model does not describe diurnal variations in mean arterial pressure.

Parameter estimation

PK parameters were estimated by fitting the imarikiren concentration clinical data using maximum likelihood estimation. PK parameters were then fixed, and PD parameters were estimated by fitting PRA and PRC longitudinal data. In addition, during this fitting, the parameter $A_{AT1,ren}$ describing the feedback of AT1-bound AngII on renin secretion was re-estimated. All other parameters of the RAAS submodule and larger cardio-renal model were fixed to calibrated values obtained from prior work [17].

Genetic algorithm (GA) optimization was used to minimize the cost function arising from the sum of squared residuals of PRA and PRC for all time points and doses. To allow comparable contributions of the residuals from the two biomarkers, log transformed PRC values were used.

Simulation of the blood pressure response in hypertensive virtual patients

To evaluate the expected trough mean arterial pressure response to imarikiren, and to benchmark it against other RAAS-targeting therapies, a cohort of hypertensive virtual patients were generated as described previously [17]. Treatment administration of each dose of imarikiren, as well as approved doses of mono- and combination RAAS therapies, were simulated for 8 weeks, and the change in trough mean arterial pressure after 8 weeks was predicted.

Software

The model was implemented and parameter estimation was conducted in R 3.1.2 using the package RxODE (https://cran.r-project.org/web/packages/RxODE/index.html), a package for simulating differential equation pharmacometric models in R [22].

Results

Time profile of imarikiren and dose-dependent renin inhibition

Estimated model parameters are given in Table 1. In order to fit the data, no changes were required to the previously developed RAAS pathway model structure. Apart from drug-specific PD parameters IC50 and k_{del}, only one parameter was re-estimated: the parameter $A_{AT1,ren}$ describing the strength of the feedback of AT1-bound AngII on renin secretion. This parameter was re-estimated to be 0.79, slightly lower than previously estimated value of 0.9.

Figure 2 shows the model fit to the observed PK, PRA, and PRC responses to single doses of imarikiren at 5, 10, 25, 50, 100 and 200 mg. The model describes well both the magnitude and time courses of the PK time profiles as well as the PRA and PRC responses. The model captures the rapid decline of PRA and concomitant rise in PRC with rapid PRA inhibition. It also captures the progressive increase in duration of PRA suppression with increasing doses. Since circadian variation in renin secretion was not modeled, the model is unable to reproduce the rise in PRA at 6 h in the placebo group. Thus, the model may

Table 1 Estimated model parameters. All other model parameters were fixed to previously calibrated values [16–18]

Parameter	Description	Value	%RSE
k_a	Oral absorption rate constant	3.57/h	14.5
k_e	Elimination rate constant	0.23/h	16.2
k_{12}	Intercompartmental rate constant	0.053/h	60.3
k_{21}	Intercompartmental rate constant	0.102/h	144
$V_{central}$	Volume of the central compartment	76.8 L	4.7
k_{del}	Rate constant for time lag of drug action or biophase effect	0.169/h	17.5
$IC50$	Effective compound concentration that produces 50% of the maximum effect on PRA inhibition	2.5 ng/mL	18.8
$A_{AT1,ren}$	Exponent parameter defining the magnitude of the AT1-bound AngII-induced renin secretion feedback.	0.79	44.7

underestimate the degree of renin suppression during times of circadian elevation. The aldosterone clinical data was highly variable, but the small reduction in aldosterone predicted by the model is consistent with the observed data.

Figure 3 further illustrates the clinically observed and model-fitted exposure–response relationship. PRA is clearly suppressed as imarikiren concentration increased (Fig. 3, left), while PRC increases with exposure. There is some hysteresis in the PRC response due to the delay between exposure, renin inhibition, and renin secretion. There was also a weak trend toward reduced aldosterone at higher drug concentrations.

Prediction of dose-dependent imarikiren-induced AT1-bound AngII reduction

Regardless of the mode of RAAS suppression, the physiologic effects of RAAS suppression depend on the degree to which AT1-bound AngII is suppressed, since AngII binding to the AT1 receptor drives the downstream effect on the renal vasculature, tubular reabsorption, and aldosterone release. Figure 4 shows the simulated percent reduction of AT1-bound AngII from baseline for 14 days daily administration of imarikiren for all doses. For each dose, AT1-bound AngII falls rapidly and oscillates within a narrow range. The lower panel of Fig. 4 shows the simulated dose–response curve for day 14 trough AT1-bound AngII suppression. The predicted degree of suppression ranged from about 82–98% as dose increased from 5 to 200 mg, with little additional suppression as the dose increased above 100 mg.

Benchmarking the PRA, PRC, and AT1-bound AngII response to imarikiren with other RAAS therapies

We previously showed that the model was able to reproduce the observed trough changes in PRA and PRC (as placebo adjusted change from baseline, composite mean of available published data for each therapy) in response to multiple RAAS monotherapies, and was able to predict the response to dual-RAAS therapy [17]. All parameter values for these therapies were taken from this previous publication, and were not reestimated here. In the present study, we benchmarked trough changes in PRA and PRC with imarikiren against other RAAS-blocking antihypertensive agents studied in [17], as shown in Fig. 5. As expected, PRA is reduced for renin inhibitors (aliskiren and imarikiren) but increased with all other RAAS monotherapies. PRC is increased with all treatments. The magnitude of the rise in PRC with imarikiren is comparable to that of the dual-RAAS combination of aliskiren 300 mg and valsartan 320 mg—the highest approved doses of these drugs.

Figure 6 shows the simulated degree of trough AT1-bound AngII suppression with imarikiren, compared to other RAAS monotherapies and dual-RAAS therapy. Except for 5 mg dose, the simulated AT1-bound AngII reduction with imarikiren was higher than any of the monotherapies. For the 25 mg dose and higher, the predicted AT1-bound AngII suppression was comparable to the combination of aliskiren 300 mg and valsartan at 320 mg.

Benchmarking the trough mean arterial pressure response to imarikiren

Blood pressure reduction is a physiological consequence of reduced vascular resistance and increased sodium excretion resulting from AT1-bound AngII suppression. In the cardio-renal QSP model, the blood pressure response to AT1-bound AngII suppression has previously been calibrated by fitting the trough mean arterial pressure reduction observed with RAAS monotherapies, and validated by simulating these therapies in combination with other RAAS therapies, with the diuretic hydrochlorothiazide, or with the calcium channel blocker amlodipine [17]. Blood pressure reduction with imarikiren in hypertensive patients has not yet been reported. In this study, we used the cardio-renal QSP model to predict the expected reduction in trough mean arterial pressure with imarikiren at steady-state (after 8 weeks of

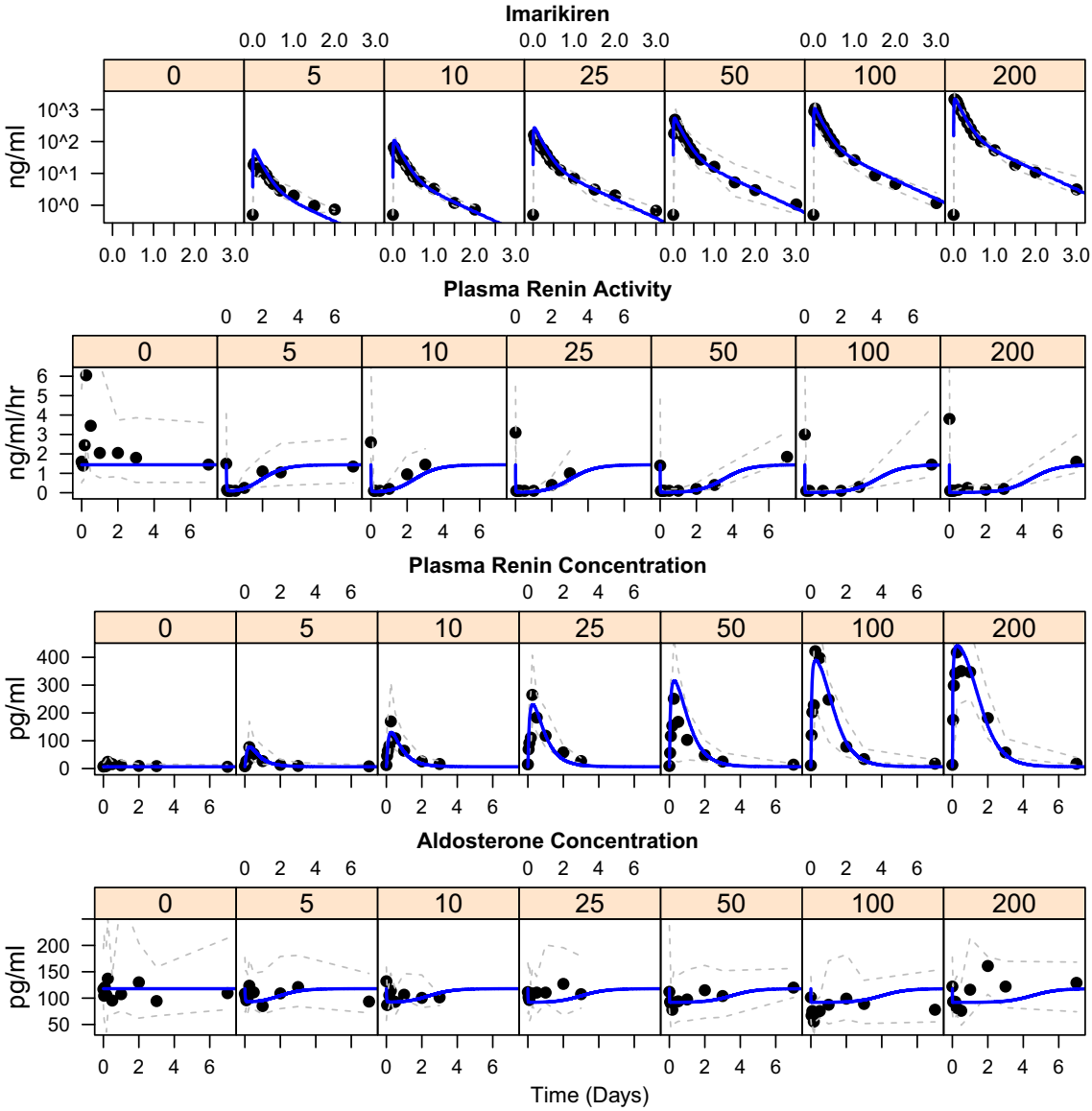

Fig. 2 Plasma concentration–time profile of imarikiren for doses ranging from 5 to 200 mg (top row). Pharmacodynamics response of renin inhibition as shown by PRA (second row), PRC (third row), and aldosterone (fourth row). Panel labels indicate the dose in mg. Solid blue curves represent model fit for the typical individual and filled circles represent clinical data. The dashed gray curves in the figure represent the 5 and 95% quantiles of the clinical data (Color figure online)

simulation time), based on the simulated RAAS suppression described above. As shown in Fig. 7, the model predicts that the steady-state MAP reduction with 10 mg imarikiren will be comparable to that achieved with the highest doses of other RAAS therapies (aliskiren, valsartan, losartan, irbesartan, candeartan, enalapril). The higher doses may achieve MAP reductions comparable to those of dual-RAAS therapies.

Discussion

In this study, we used a model-based approach to quantify RAAS suppression with the DRI imarikiren, and to benchmark the degree of RAAS supression and model-predicted blood-pressure regulation against other RAAS-blocking therapies. PK and PD parameteres that are specific to imarikiren, as well as the parameter defining the magnitude of the feedback on renin-secretion $A_{AT1,ren}$, were estimated. The estimated IC50 for renin suppression with imarikiren of 0.19 ng/mL was very similar to the measured in vitro IC50 value of 0.113 ng/mL. $A_{AT1,ren}$ was

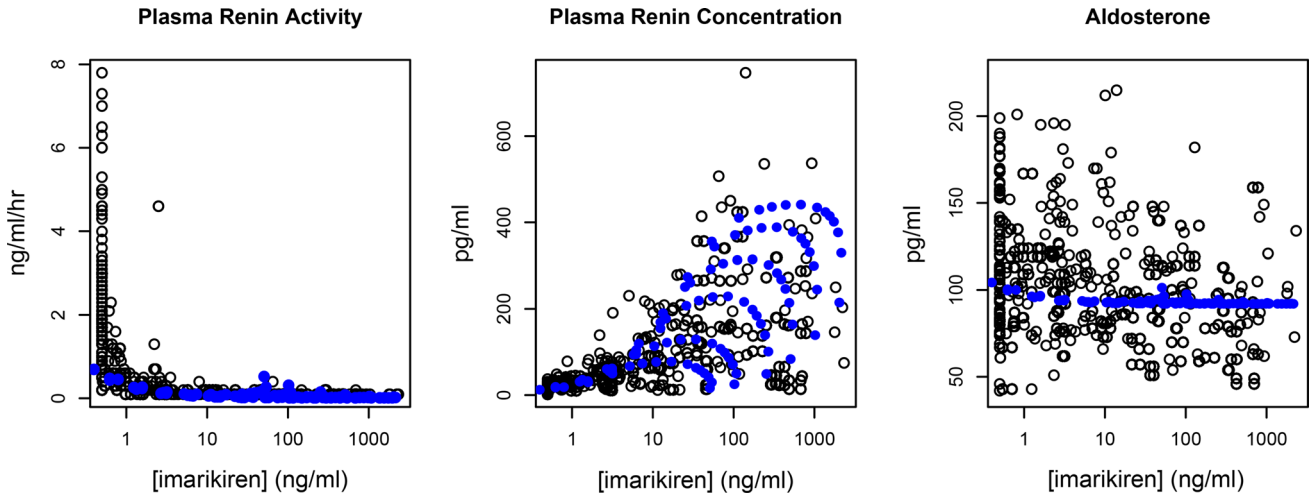

Fig. 3 Imarikiren exposure–response for PRA (left), PRC (middle), and aldosterone (right). Open black circles are clinical data, and closed blue circles are model simulations at the same dose and time points as the clinical data

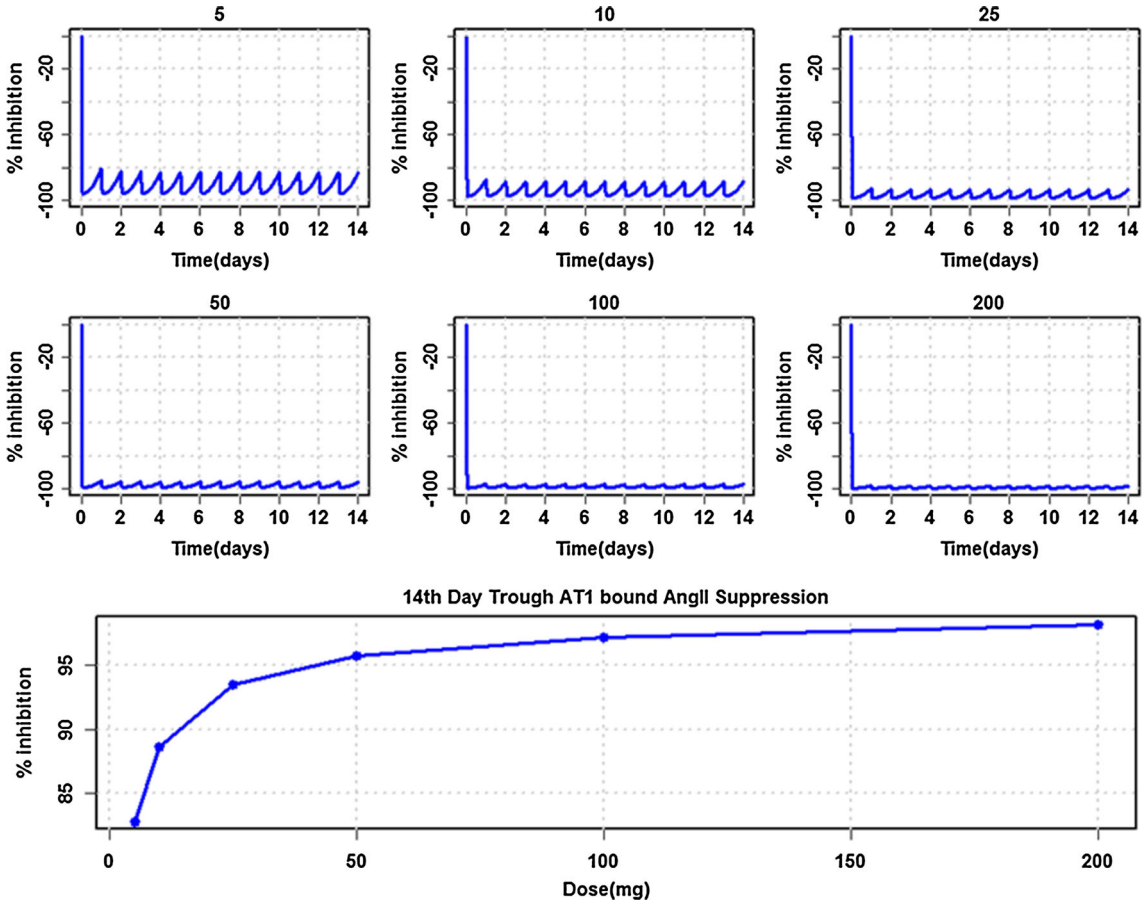

Fig. 4 Top two rows: Simulated percent reduction of AT1-bound AngII for daily administration of 5, 10, 25, 50, 100 and 200 mg doses (as indicated at top of each plot) of imarikiren. Bottom row: model-predicted dose–response curve for 14-day trough AT1-bound AngII suppression with imarikiren

estimtaed to be 0.79, slightly less but similar to the value of 0.9 estimated in our previous study [17]. This small difference could be due to differences between study populations. Our previous calibration utilized data from both healthy volunteers and hypertensive patients, while the current study included only healthy volunteers. It is possible that hypertensive patients have an overactive feedback response, compared to healthy volunteers. No other

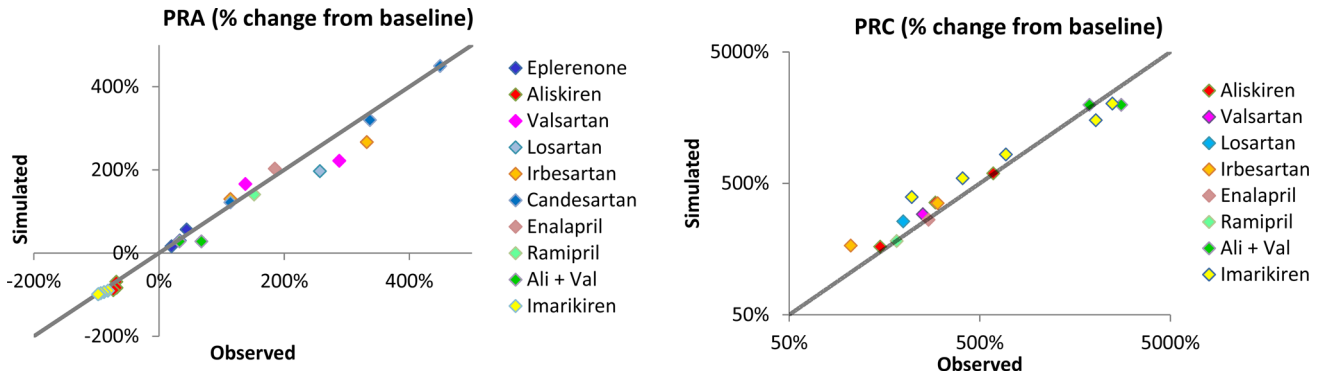

Fig. 5 Simulated versus experimentally observed trough changes in PRA (left panel) and PRC (right panel), for multiple RAAS antihyperthensive therapies. All data are placebo-adjusted change from baseline to pre-dose on the final reported study day. Imarikiren data are from this study. Data for other therapies are the composite mean of available published data for each therapy as described in Ref. [17]. The solid line in each panel is the 1:1 ratio line of perfect agreement between observed and simulated responses

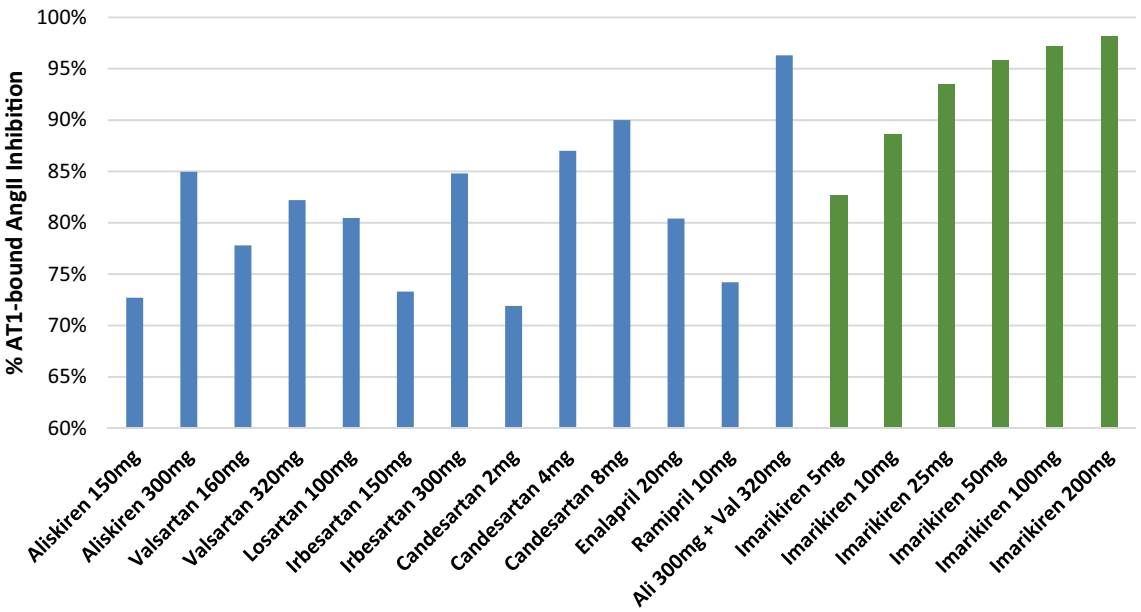

Fig. 6 Comparison of model-predicted trough AT1-bound AngII change from baseline with imarikiren and other RAAS therapies, alone and in combination. Data for other therapies are based on previously published data [17]. Green bars: Imarikiren; blue solid bars: other RAAS therapies (Color figure online)

model parameters were changed, and the model was able to describe both the magnitude and timecourse of the PRA and PRC responses. Thus, this study provides additional validation of the previous model.

Our results indicate that AT1-bound AngII suppression with low doses (below 25 mg) of imarikiren is comparable to that of the highest approved dose of aliskiren (300 mg) as well as many other RAAS monotherapies. Medium to high doses (25 mg/kg and above) of imarikiren suppressed AT1-bound AngII to a greater degree than other monothrapies analyzed, and the degree of suppression for these doses was comparable to that of dual-RAAS therapies. Very little additional suppression was observed as the dose of imarikiren increased from 100 to 200 mg.

Blood pressure reduction with imarikiren treatment in hypertensive patients has not yet been reported, but we utilized the model to predict the expected blood pressure response in virtual hypertensive patients, and compared this response to predictions with other RAAS therapies. Lower doses of imarikiren were predicted to lower MAP similar to other RAAS monotherapies, while the prediction for doses of 50 mg or higher were predicted to be comparable to RAAS combination therapy.

In drug development, efficacy biomarkers obtained in phase I studies are often used to infer expected efficacy and to make dosing, go/no go, and other decisions for phase II. This analysis demonstrates how a QSP model can be used to make quantitive predictions of a phase II endpoint like

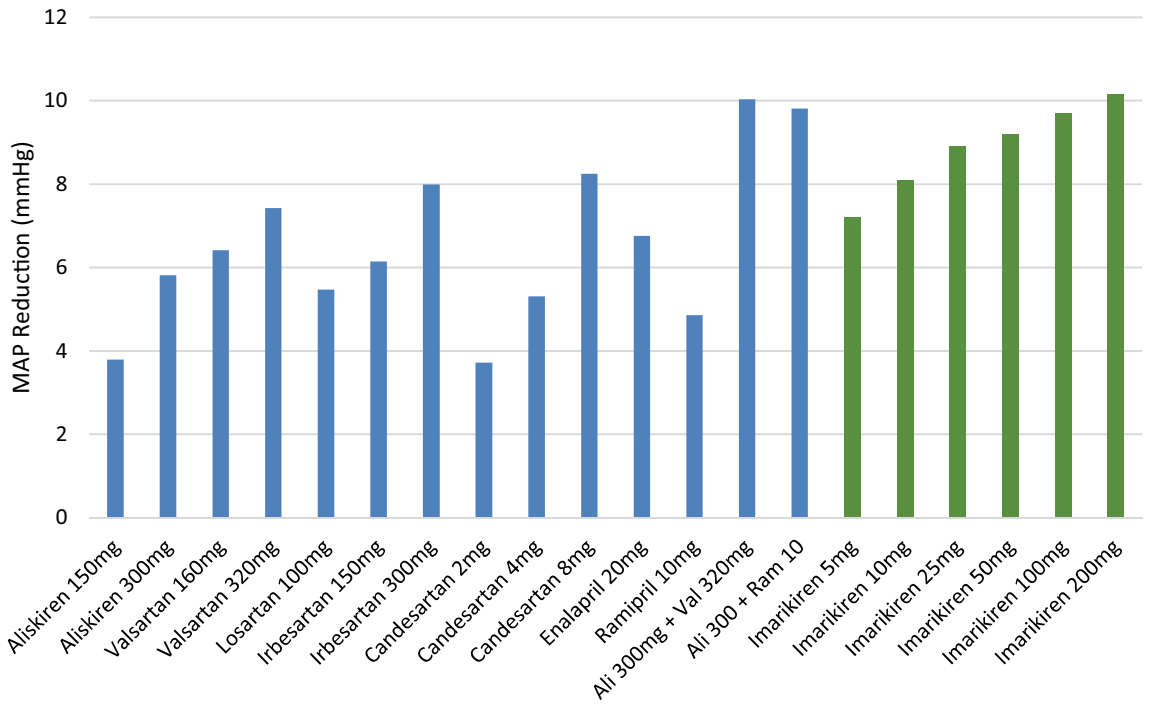

Fig. 7 Benchmarking imarikiren against other RAAS mono- and dual therapies: model-predicted reductions in trough mean arterial pressure at steady-state with imarikiren, compared with preivously calibrated and validated model predicted reductions with other RAAS therapies [17]

blood pressure reduction utilizing phase I biomarkers like PRA and PRC, and to benchmark efficacy of a new compound against existing compounds. Although the predictions must ultimately be validated with measurements in clinical trials, these early predictions can help development teams make more informed and objective decisions based on the available data for both new and existing compounds.

Limitations

While the timecourse of RAAS suppression with imarikiren was evaluated using detailed timecourse clinical measures of imarikiren-induced changes, comparisons with other RAAS blocking agents were made using trough measures only, since PRA and PRC measurements in the literature are most commonly reported using trough values. It is possible that other RAAS monotherapies suppress the RAAS to similar degrees but may not maintain the suppression through trough, perhaps obscuring the degree of suppression in some of these drugs. Similarly, in this study we predicted the steady-state blood pressure reduction, but did not attempt to account for the timecourse of reduction or the daily blood pressure dynamics.

This analysis did not consider the chronobiology of the RAAS [23–25]. Other have previously elegantly modeled circadian dynamics of the RAAS [3]. However, the current study lacked sufficient time resolution in the clinical data to adequately capture circadian effects. Because the primary goal was to benchmark trough RAAS suppression and MAP reduction with existing therapies, we do not expect that circadian effects would significantly impact the conclusions. However, if this model were used to address other questions such as the morning vs evening dosing or differences in 24 h blood pressure control, circadian effects would become important. For such questions, the current model would need to be extended using an approach similar to that of Mochel et al. [25].

Calibration and validation of other RAAS therapies were based on data taken from a number of studies, and systematic reviews like Cochrane were used when available, as described previously [17]. Weighted composite means were calculated when multiple studies are available. While a strength of QSP modeling lies in the incorporation of data from multiple studies into a single quantitative framework, it is also possible that differences in study populations between studies may influence the observed PRA, PRC, and blood pressure responses, and thus may also influence the model calibration and predictions. The model also was calibrated using median data, and does not account for individual variability.

Conclusion

This study provides validation for our previously developed RAAS pathway model, and illustrates the application of QSP modeling to predict phase II endpoints based on

phase I data. Our analysis indicates that low doses of imarikiren are comparable to current RAAS monotherapies, and that at higher doses, RAAS suppression may be equivalent to that of existing dual-RAAS blockers.

Funding This study was supported by Takeda Pharmaceuticals.

Compliance with ethical standards

Conflict of interest G. Lahu and M. Vakilynejad are/were employees of Takeda Pharmaceutical Corporation.

References

1. Morris BJ, Catanzaro DF (1981) Biosynthesis of preprorenin and intracellular conversion of prorenin to renin. Clin Exp Pharmacol Physiol 8(5):441–445
2. Campbell DJ (2008) Critical review of prorenin and (pro)renin receptor research. Hypertension 51(5):1259–1264. https://doi.org/10.1161/HYPERTENSIONAHA.108.110924
3. Mochel JP, Danhof M (2015) Chronobiology and pharmacologic modulation of the renin-angiotensin-aldosterone system in dogs: what have we learned? Rev Physiol Biochem Pharmacol 169:43–69. https://doi.org/10.1007/112_2015_27
4. Fyhrquist F, Metsarinne K, Tikkanen I (1995) Role of angiotensin II in blood pressure regulation and in the pathophysiology of cardiovascular disorders. J Hum Hypertens 9(Suppl 5):S19–S24
5. Mehta PK, Griendling KK (2007) Angiotensin II cell signaling: physiological and pathological effects in the cardiovascular system. Am J Physiol Cell Physiol 292(1):C82–C97. https://doi.org/10.1152/ajpcell.00287.2006
6. Matavelli LC, Siragy HM (2015) AT2 receptor activities and pathophysiological implications. J Cardiovasc Pharmacol 65(3):226–232. https://doi.org/10.1097/fjc.0000000000000208
7. Peluso AA, Santos RA, Unger T, Steckelings UM (2017) The angiotensin type 2 receptor and the kidney. Curr Opin Nephrol Hypertens 26(1):36–42. https://doi.org/10.1097/mnh.0000000000000289
8. Singh KD, Karnik SS (2016) Angiotensin receptors: structure, function, signaling and clinical applications. J Cell Signal. https://doi.org/10.4172/jcs.1000111
9. Ma TK, Kam KK, Yan BP, Lam YY (2010) Renin-angiotensin-aldosterone system blockade for cardiovascular diseases: current status. Br J Pharmacol 160(6):1273–1292. https://doi.org/10.1111/j.1476-5381.2010.00750.x
10. Shafiq MM, Menon DV, Victor RG (2008) Oral direct renin inhibition: premise, promise, and potential limitations of a new antihypertensive drug. Am J Med 121(4):265–271. https://doi.org/10.1016/j.amjmed.2007.11.016
11. Sealey JE, Laragh JH (2007) Aliskiren, the first renin inhibitor for treating hypertension: reactive renin secretion may limit its effectiveness. Am J Hypertens 20(5):587–597. https://doi.org/10.1016/j.amjhyper.2007.04.001
12. Nussberger J, Wuerzner G, Jensen C, Brunner HR (2002) Angiotensin II suppression in humans by the orally active renin inhibitor Aliskiren (SPP100): comparison with enalapril. Hypertension 39(1):E1–E8
13. Stanton A, Jensen C, Nussberger J, O'Brien E (2003) Blood pressure lowering in essential hypertension with an oral renin inhibitor, aliskiren. Hypertension 42(6):1137–1143. https://doi.org/10.1161/01.hyp.0000101688.17370.87
14. Imaeda Y, Tokuhara H, Fukase Y, Kanagawa R, Kajimoto Y, Kusumoto K, Kondo M, Snell G, Behnke CA, Kuroita T (2016) Discovery of TAK-272: a novel, potent, and orally active renin inhibitor. ACS Med Chem Lett 7(10):933–938. https://doi.org/10.1021/acsmedchemlett.6b00251
15. Chappell MC (2016) Biochemical evaluation of the renin-angiotensin system: the good, bad, and absolute? Am J Physiol Heart Circ Physiol 310(2):H137–H152. https://doi.org/10.1152/ajpheart.00618.2015
16. Lo A, Beh J, de Leon H, Hallow KM, Ramakrishna R, Rodrigo M, Sarkar A, Sarangapani R, Georgieva A (2011) Using a systems biology approach to explore hypotheses underlying clinical diversity of the renin angiotensin system and the response to antihypertensive therapies. In: Kimko HC, Peck C (eds) Clinical trial simulations. Springer, New York
17. Hallow KM, Lo A, Beh J, Rodrigo M, Ermakov S, Friedman S, de Leon H, Sarkar A, Xiong Y, Sarangapani R, Schmidt H, Webb R, Kondic AG (2014) A model-based approach to investigating the pathophysiological mechanisms of hypertension and response to antihypertensive therapies: extending the Guyton model. Am J Physiol Regul Integr Comp Physiol 306(9):R647–R662. https://doi.org/10.1152/ajpregu.00039.2013
18. Hallow KM, Gebremichael Y (2017) A quantitative systems physiology model of renal function and blood pressure regulation: model description. CPT Pharmacometri Syst Pharmacol 6(6):383–392. https://doi.org/10.1002/psp4.12178
19. Hong Y, Dingemanse J, Mager DE (2008) Pharmacokinetic/pharmacodynamic modeling of renin biomarkers in subjects treated with the renin inhibitor aliskiren. Clin Pharmacol Ther 84(1):136–143. https://doi.org/10.1038/sj.clpt.6100495
20. Hallow KM, Gebremichael Y (2017) A quantitative systems physiology model of renal function and blood pressure regulation: application in salt-sensitive hypertension. CPT Pharmacometr Syst Pharmacol 6(6):393–400. https://doi.org/10.1002/psp4.12177
21. Hallow KM, Gebremichael Y, Helmlinger G, Vallon V (2017) Primary proximal tubule hyperreabsorption and impaired tubular transport counterregulation determine glomerular hyperfiltration in diabetes: a modeling analysis. Am J Physiol Renal Physiol 312(5):F819–F835. https://doi.org/10.1152/ajprenal.00497.2016
22. Wang W, Hallow KM, James DA (2016) A tutorial on RxODE: simulating differential equation pharmacometric models in R. CPT Pharmacometr Syst Pharmacol 5(1):3–10. https://doi.org/10.1002/psp4.12052
23. Cugini P, Murano G, Lucia P, Letizia C, Scavo D, Halberg F, Cornelissen G, Sothern RB (1985) Circadian rhythms of plasma renin activity and aldosterone: changes related to age, sex, recumbency and sodium restriction. Chronobiologic specification for reference values. Chronobiol Int 2(4):267–276
24. Hermida RC, Ayala DE, Mojon A, Fernandez JR (2010) Effects of time of antihypertensive treatment on ambulatory blood pressure and clinical characteristics of subjects with resistant hypertension. Am J Hypertens 23(4):432–439. https://doi.org/10.1038/ajh.2009.260
25. Mochel JP, Fink M, Bon C, Peyrou M, Bieth B, Desevaux C, Deurinck M, Giraudel JM, Danhof M (2014) Influence of feeding schedules on the chronobiology of renin activity, urinary electrolytes and blood pressure in dogs. Chronobiol Int 31(5):715–730. https://doi.org/10.3109/07420528.2014.897711